The 2015 World Congress on
Advances in Structural Engineering and Mechanics (ASEM15)
Incheon, Korea, August 25-29, 2015

Numerical analysis for the fire-induced progressive collapse of a RC frame structure

Mengzhu Diao[1)], Lanping Qian[2)], Yi Li[3)], *Xinzheng Lu[4)] and Hong Guan[5)]

[1), 2), 3)] *Key Laboratory of Urban Security and Disaster Engineering of Ministry of Education, Beijing Collaborative Innovation Center for Metropolitan Transportation, Beijing University of Technology, Beijing 100124, China*
[4)] *Key Laboratory of Civil Engineering Safety and Durability of Ministry of Education, Department of Civil Engineering, Tsinghua University, Beijing 100084, China*
[5)] *Griffith School of Engineering, Griffith University Gold Coast Campus, Queensland 4222, Australia*
[4)] *luxz@tsinghua.edu.cn*

ABSTRACT

In order to investigate the fire-induced progressive collapse of reinforced concrete (RC) frame structures, a fiber beam model for RC beams and columns and a layered shell model for RC slabs are developed. In these models, the sections at each integral point are divided into some fibers or layers. Different materials are assigned to different fibers and layers to consider the distribution of reinforcing steel and concrete. The relation between the deformation of the elements and the strains of the fibers or layers is defined following the assumption of “plane section remains plane”. To consider the effect of high temperature, the thermal-mechanical coupled constitutive laws are adopted for the concrete and steel in the fibers and layers. Temperature-stress paths are discretized into several sub-increments. Various strain components induced by the coupled action of temperature and stress, i.e. the stress strain, the free thermal expansion strain, the short-term high-temperature creep strain and the transient thermal strain, are calculated within each sub-increment. Through a series of experiments, the accuracy and efficiency of the models in simulating the behavior of RC beams, columns and slabs in fire are validated. Then, the failure criteria and the deactivation of the elements are adopted in the models, so the influence of internal force redistribution induced by elemental fracture on the mechanical response of the whole structure is taken into

---

[1)2)] Graduate Student
[3)] Assistant Professor
[4)] Professor
[5)] Associate Professor

consideration. At last, the collapse simulation of a whole RC frame structure subjected to fire shows the effect of the proposed model.

1. INTRODUCTION

The progressive collapse of a building is initiated by an event that causes the local damage that the structural system can not absorb or contain, and the subsequently propagates throughout the structural system or a major portion of it, leading to a final damage state that is disproportionate to the local damage that initiated it (Ellingwood 2006). Progressive collapse is the global behavior of the whole structure, which is suitable to be studied by numerical approaches. There are following three key points to address when simulating the fire-induced progressive collapse of structures: (1) dynamic fire field inside the building and uneven temperature distribution along the structural members; (2) degradation of material strength and stiffness at high temperature; (3) internal force redistribution of the structural systems caused by the damage and failure of local members. Considering the workload of the parametric analysis during the scientific research and engineering design, the numerical approach of the fire-induced collapse should be both highly accurate and efficient.

To simulate the reinforced concrete (RC) frame structure subjected to fire with a high accuracy and efficiency, this work introduces the thermal-mechanical coupled constitutive laws to simulate the behavior of RC members (including beam, column and slab) at high temperature based on the high-performance element of fiber beam and layered shell. Then the failure criteria and the element deactivation technique are incorporated to the model to consider the element failure. Thus, an efficient numerical approach to model the global structural fire-induced progressive collapse behavior has been established. Finally, a series of experiments of members are used to validate the accuracy of the proposed model and the application of the model on an 8-story RC frame case shows its capacity of the fire-induced collapse simulation for the whole structural system.

2. THERMAL-MECHANICAL COUPLED MATERIAL CONSTITUTE LAW

2.1 The strains at high temperature

The total strain ε^{c} of concrete under high temperature consists of following 4 parts: the stress strain $\varepsilon^{c}_{\sigma}(T, \sigma)$, the free thermal expansion strain $\varepsilon^{c}_{th}(T)$, the short-term high-temperature creep strain $\varepsilon^{c}_{cr}(T,\sigma,t)$ and the transient thermal strain $\varepsilon^{c}_{tr}(T,\sigma)$, in which T, σ, t represent the temperature, stress and time, respectively (Guo 2003a). Then the concrete total strain ε^{c} can be expressed by Eq. (1):

$$\varepsilon^{c} = \varepsilon_{\sigma}^{c}(T,\sigma) + \varepsilon_{th}^{c}(T) + \varepsilon_{cr}^{c}(T,\sigma,t) + \varepsilon_{tr}^{c}(T,\sigma) \quad (1)$$

Similarly, the total strain of reinforcing steel ε^{s} under high temperature is expressed as:

$$\varepsilon^{s} = \varepsilon_{\sigma}^{s}(T,\sigma) + \varepsilon_{th}^{s}(T) + \varepsilon_{cr}^{s}(T,\sigma,t) \quad (2)$$

where ε_{σ}^{s}, ε_{th}^{s}, ε_{cr}^{s} represent the stress stain, the free thermal expansion strain and the short-term creep strain of steel respectively. Different from concrete, the transient thermal strain doesn't exist in heated steel.

2.2 Temperature-stress path

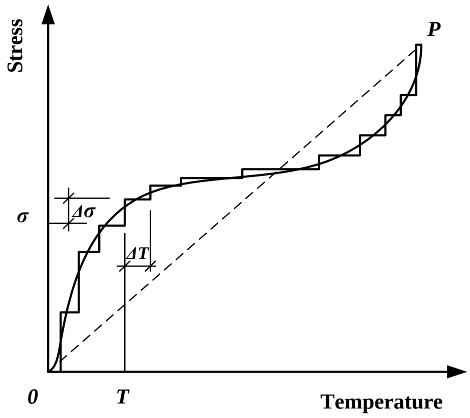

Fig. 1. Temperature-stress discretizing load path.

The material behavior at high temperature is controlled by the temperature *T* and time *t*. Hence, the material exhibits different stress-strain states under different stress-temperature paths. A random temperature-stress load path OP shown in Fig. 1 can be discretized into many temperature and stress sub-increments. The discretized path is able to approximate the real path when the sub-increments of stress and time are small enough(Guo 2003a). Within a single temperature-stress sub-increment, Path $(T, \sigma) \rightarrow (T+\Delta T, \sigma+\Delta\sigma)$ can be disassembled into two steps: $(T, \sigma) \rightarrow (T, \sigma+\Delta\sigma) \rightarrow (T+\Delta T, \sigma+\Delta\sigma)$, by which the stress and temperature can be decoupled in the computation.

2.3 Material constitutive law at high temperature

Free thermal expansion strain The free thermal expansion strain of material ε_{th}

relates only to T, so $\mathrm{d}\varepsilon_{\mathrm{th}}$ is calculated though Path $(T, \sigma+\Delta\sigma) \rightarrow (T+\Delta T, \sigma+\Delta\sigma)$. The thermal expansion model of concrete and steel proposed by Guo and Shi (Guo 2003a) is adopted in this work as shown in Eq. (3).

$$\mathrm{d}\varepsilon_{\mathrm{th}}^{\mathrm{c}} = \begin{cases} 56T \times 10^{-9} dT & T < 655°C \\ 0 & T \geq 655°C \end{cases} \tag{3}$$

$$\mathrm{d}\varepsilon_{\mathrm{th}}^{\mathrm{c}} = \begin{cases} 56T \times 10^{-9} dT & T < 655°C \\ 0 & T \geq 655°C \end{cases} \tag{4}$$

in which $\mathrm{d}\varepsilon_{\mathrm{th}}^{\mathrm{c}}$ and $\mathrm{d}\varepsilon_{\mathrm{th}}^{\mathrm{s}}$ are the incremental free thermal expansion strain of concrete and steel, respectively.

<u>Short-term creep strain</u> The short-term creep incremental strain $\mathrm{d}\varepsilon_{\mathrm{cr}}^{\mathrm{c}}$ of concrete also adopts the model proposed by Guo and Shi (Guo 2003a) as follows:

$$d\varepsilon_{\mathrm{cr}}^{\mathrm{c}} = \frac{\sigma}{f_{\mathrm{c}}^{\mathrm{T}}} \left(e^{\frac{6T}{1000}} - 1 \right) \frac{30 \times 10^{-6}}{\sqrt{t^{\mathrm{eq}} t_0}} dt \tag{5}$$

$$t^{\mathrm{eq}} = \left[\frac{\varepsilon_{\mathrm{cr}}^{\mathrm{c}} \times 10^{6}}{\frac{\sigma}{f_{\mathrm{c}}^{\mathrm{T}}} \left(e^{\frac{6T}{1000}} - 1 \right) \times 60} \right] \tag{6}$$

where $f_{\mathrm{c}}^{\mathrm{T}}$ is the compressive strength of concrete at high temperature, t_0 is a constant parameter (120 min), and t^{eq} is the equivalent time.

The thermal creep strain of steel is modeled according to the work of Williams(1983) as:

$$\dot{\varepsilon}_{\mathrm{cr}}^{\mathrm{s}} = b_1 \coth^2 (b_2 \varepsilon_{\mathrm{cr}}^{\mathrm{s}}) \tag{7}$$

where $\dot{\varepsilon}_{\mathrm{cr}}^{\mathrm{s}}$ is the thermal creep ratio of steel, b_1 and b_2 are material constants.

Concrete thermal transient strain   The transient thermal strain $\varepsilon_{\mathrm{tr}}$ is a special strain component in concrete. According to its definition, concrete produces the transient strain only at high temperature under compression (Guo 2003a). $\mathrm{d}\varepsilon_{\mathrm{tr}}^{\mathrm{c}}$ can be calculate though Path $(T,\sigma+\Delta\sigma)\rightarrow(T+\Delta T,\sigma+\Delta\sigma)$ within a single temperature-stress sub-increment as (Guo 2003a):

$$\mathrm{d}\varepsilon_{\mathrm{tr}}^{\mathrm{c}}=\frac{\sigma}{f_{\mathrm{c}}^{\mathrm{T}}}\left[144\left(\frac{T}{1000}-1\right)\right]\times10^{-6}dT \tag{8}$$

Stress-strain model under constant temperature   The stress-strain models of concrete and reinforcing steel at constant temperature are given by Bratina et al. (2007). The main mechanical characteristics varying with temperature (such as the elasticity modulus, yield strength, ultimate strength, yield strain and ultimate strain) are defined using the model proposed by Guo and Shi (Guo 2003a) as follows:

$$\frac{f_{\mathrm{c}}^{\mathrm{T}}}{f_{\mathrm{c}}}=\frac{1}{1+18(\frac{T}{1000})^{5.1}} \tag{9}$$

$$\frac{E_0^{\mathrm{T}}}{E_0}=0.83-0.0011T \tag{10}$$

$$\frac{\varepsilon_{\mathrm{p}}^{\mathrm{T}}}{\varepsilon_{\mathrm{p}}}=1+5(\frac{T}{1000})^{1.7} \tag{11}$$

$$\frac{f_{\mathrm{t}}^{\mathrm{T}}}{f_{\mathrm{t}}}=1-\frac{T}{1000} \tag{12}$$

where f_{c}, E_0, ε_{p}, f_{t} represent the ultimate compressive strength, the initial elastic modulus, the ultimate compressive strain and the tensile strength of concrete at ambient temperature, respectively; $f_{\mathrm{c}}^{\mathrm{T}}$, E_0^{T}, $\varepsilon_{\mathrm{p}}^{\mathrm{T}}$, $f_{\mathrm{t}}^{\mathrm{T}}$ represent the ultimate compressive strength, the initial elastic modulus, the ultimate compressive strain and the tensile strength of concrete at high temperature respectively.

$$\frac{f_y^T}{f_y} = \frac{1}{1 + 24(\frac{T}{1000})^{4.5}} \tag{13}$$

$$\varepsilon_y^T = \phi\varepsilon_y \tag{14}$$

$$\varepsilon_{su}^T = 0.16 - 0.23\left(\frac{T}{1000}\right) \geq 0.02 \tag{15}$$

where f_y, ε_y represent the yield strength and the yield strain of reinforcing steel at ambient temperature, respectively; f_y^T, ε_y^T, ε_{su}^T represent the yield strength, the yield strain and the ultimate strain of reinforcing steel at high temperature, respectively; ϕ equals 1.20.

3. THE FIBER BEAM MODEL FOR BEAMS AND COLUMNS

3.1 Basic principle

Beams and columns are the main load-bearing members of RC frame structures. The fiber beam model can simulate the mechanical properties of these members accurately and efficiently (Ye 2006). In the model, the cross-sections are divided into many small fibers. The uniaxial stress-strain relation of different materials can be assigned to different fibers to represent the mechanical characteristics of composite structure. The deformation of the cross-sections follows the assumption of "plane section remains plane". An independent parameter, i.e. temperature, is incorporated with each fiber by which the non-uniform temperature distribution along the structural members can be considered.

3. 2 Validation of the fiber beam model

<u>Plain concrete columns exposed to four-side fire</u> Nan (1994) conducted a fire test on a series of plain concrete columns subjected to axial compression with different initial load ratio (i.e. 0.0, 0.2, 0.4 and 0.6), as shown in Fig. 2(a). The simulation results of the fiber beam model agree well with the test data (see Fig. 2(b)).

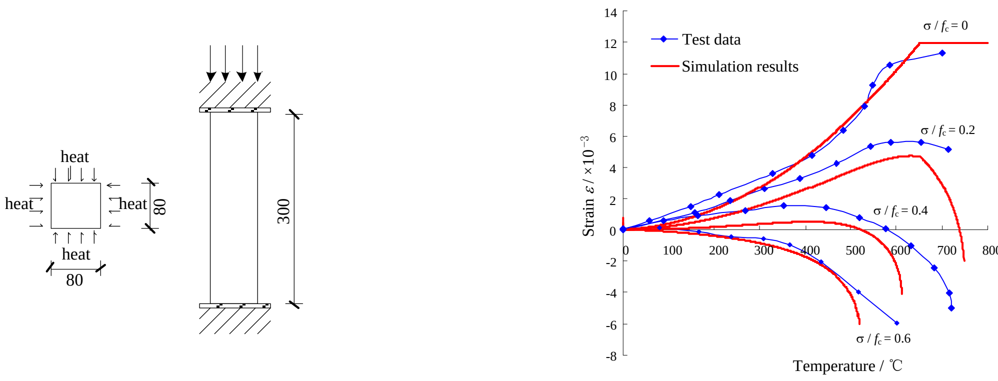

(a) Experimental scheme (b) Experimental simulation

Fig. 2. Simulation for plain concrete columns exposed to four-side fire.

<u>RC column exposed to four-side fire</u> Lie (1993) conducted a series of full-scale fire resistance tests on RC columns exposed to four-side fire. This work selects one member as a typical example for model validation, as shown in Fig. 3(a). The sectional temperature field analyzed by MSC.MARC is shown in Fig. 3(b). The experimental and predicted temperatures on the member surface are very close. However, some discrepancies are observed in the internal area before the temperature approaching 100°C. This is because the temperature field analysis employs the thermal parameters (Lie 1993, CEN 2004a, CEN 2004b), in which the heat loss, via the moisture evaporation in concrete at 100 ºC, is converted into the additional equivalent thermal capacity of concrete, between 0ºC and 100ºC. In doing so, the discontinuation of the thermal capacity of concrete, due to the moisture evaporation at 100ºC, is prevented which, in turn, facilitates the convergence of numerical computation. The process

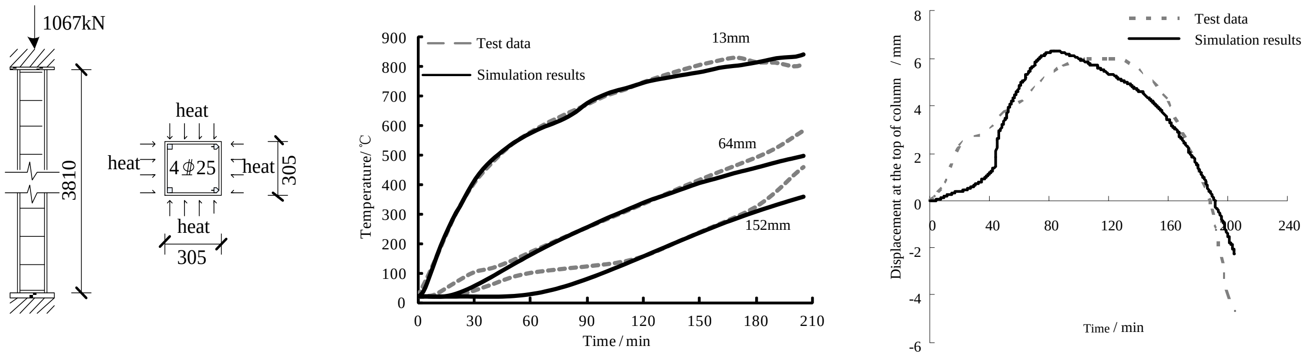

(a)Experimental scheme (b) Temperature field on the cross-section (c) Axial displacement

Fig. 3. RC column exposed to four-side fire.

inevitably results in some errors in the calculation of the temperature field below 100 ºC, but the results are accurate at a higher temperature, as shown in Figure 3. Consequently, the model can still predict the final failure time and the deformation accurately.

<u>RC column exposed to three-side fire</u> A test of RC columns exposed to three-side fire was conducted by Guo and Shi (Guo 2003a). One specimen is selected to validate the performance of the fiber beam model on simulating the mechanical behavior of RC members subjected to non-uniform fire. It can be seen in Fig. 4 that the simulated response of the column under non-uniform fire agrees well with the experimental results.

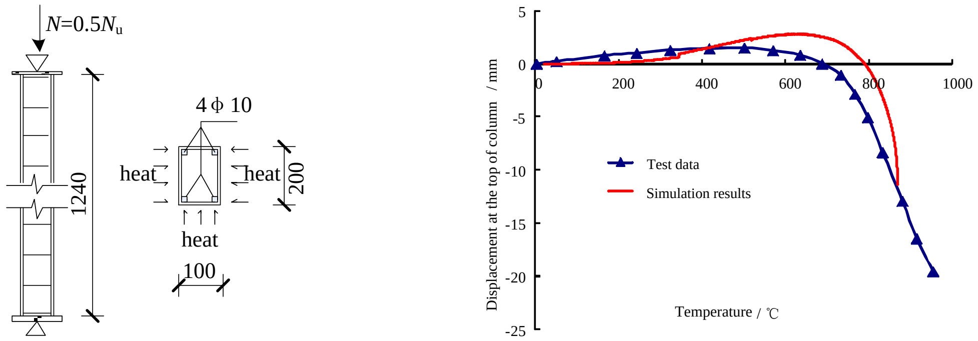

(a) Experimental scheme (b) Displacement

Fig. 4. RC column exposed to three-side fire.

4. THE LAYERED SHELL MODEL FOR SLABS

4.1 The Basic principle

The Basic principle of the layered shell model is similar to that of the fiber beam model. The layered shell model divides the shell element into many layers along the direction of thickness and each layer is assigned with different thicknesses and materials. The deformation of layers also satisfies the assumption of “plane section remains plane” (Ye 2006). Each layer is also assigned with different temperatures according to the computed results of the heat transfer analysis.

4.2 Validation of the layered shell model

<u>Simply-supported one-way slab</u> Chen (2004) conducted a fire test on three RC one-way slabs and one member (B-3) is simulated by the layered shell model as shown in Fig. 5. The specimen was simply supported at both ends and exposed to the fire from

the bottom. The temperature distribution along the thickness and the mechanical response of the specimen are shown in Fig. 5(b). The validation shows that the layered shell model integrated with thermal-mechanical coupled constitutive laws can predict the fire performance of one-way slab accurately.

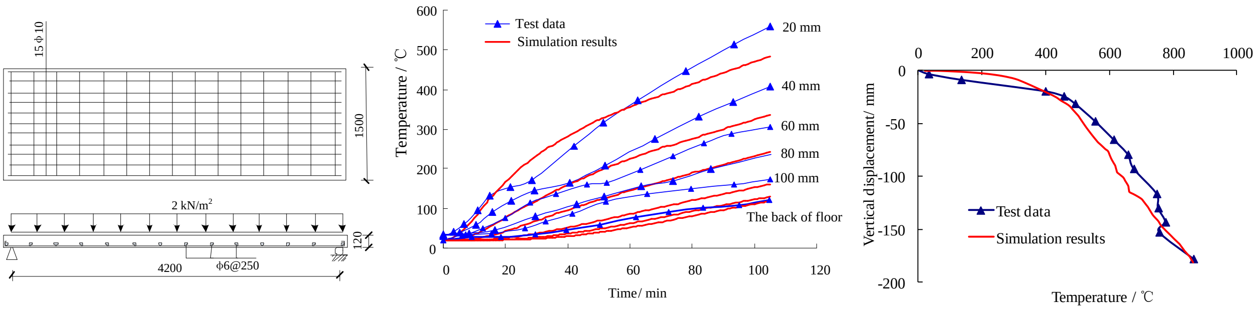

(a)Experimental scheme (b) Temperature field (c) Deformation

Fig. 5. Simply-supported one-way slab.

<u>Simply-supported two-way slabs</u> A series of simply-supported two-way slabs were tested by Lim and Wade (2002). Two specimens (DH12 and D147) are simulated using the layered shell model as shown in Fig. 6. The specimens were simply supported at four edges and were heated on the bottom. The validation also shows that the calculated temperature and deformation are consistent with the experimental results.

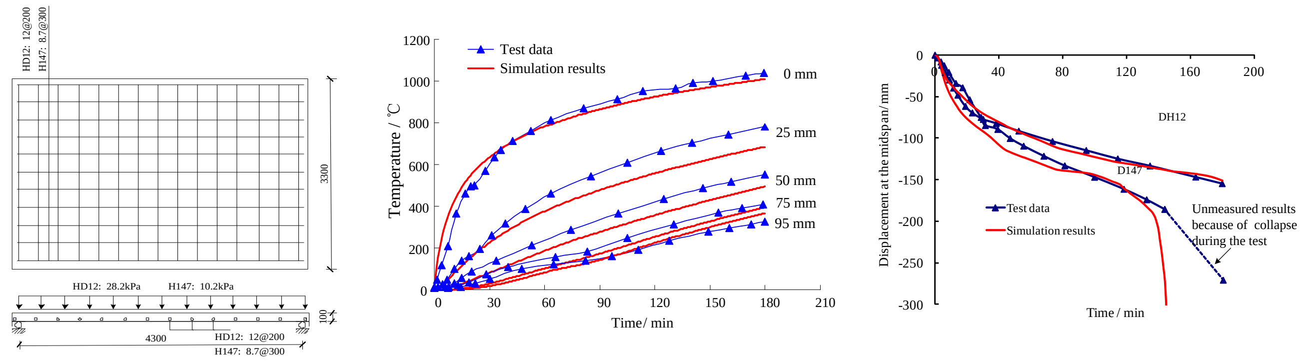

(a)Experimental scheme (b) Temperature field (c) Deformation

Fig. 6. Simply-supported two-way slabs.

4.3 Element failure criteria

During the structural collapse, damage and fracture occurred in some members, causing a redistribution of the internal forces. By establishing the appropriate failure criteria for the structural components under high temperature, the fracture of these components was simulated by using the “elemental deactivation” technique (MSC.Software Corporation 2007). For the RC columns and beams exposed to fire, the tensile failure of the reinforcement occurred when its ultimate tensile strain was reached at a high temperature. Similarly, the compressive failure of concrete occurred when its ultimate crushing strain was reached. As defined in this work, the beam or column sectional failure was reached upon the fracturing of all the steel fibers or the crushing of all the concrete fibers within that section, respectively. The RC beams exhibited bending and tensile capacities under small and large deformations, respectively, which contributed to the collapse resistance of the building (Yi 2007). Similarly, bending and compressive mechanisms also existed in the columns under small and large deformations, respectively. The failure criteria allowed the RC beams and columns to undergo both small and large deformations, but they only failed with the large deformations. When a structural member reached its failure criterion, the corresponding element was subsequently removed from the finite element model using the “elemental deactivation” technique. As a result, the internal force of the removed element was also released (MSC.Software Corporation 2007). The ultimate strains on the steel and concrete at high temperatures, suggested by Guo and Shi (Guo 2003b), were adopted in the current work to determine the failure of the material fibers.

5. APPLICATION

The simulation for an 8-story RC frame structure has been conducted to validate the developed model. The structure is designed according to the requirement of the seismic design intensity of 8 degree, i.e. the peak ground acceleration (PGA) of the design earthquake (i.e., a 10% probability of exceedance in 50 years) is 0.2g where g is the gravity acceleration.

5.1 Structure model

The plan layout of the 8-story frame structure and the number of columns are shown in Fig. 7(a). The location of fire is set in the corner bay on the fifth floor, as shown in Fig. 7(b). The elevated temperature curve adopts the HC curve suggested by the Code of Design on Building Fire Protection and Prevention (Ministry of Construction P.R.China 2006) and the duration of the fire is 10 hours. In the thermal analysis, the boundary conditions of each member under fire are as follows: the bottom fire for the slabs, the three-side fire for the frame beams (bottom and both sides) and the four-side fire for the frame columns. The proposed layered shell model and the fiber beam model are used to simulate the slabs and the beams (or columns) respectively. The slabs and the frame beams are casted together, so the layered shells and the fiber beams are coupled by using common nodes.

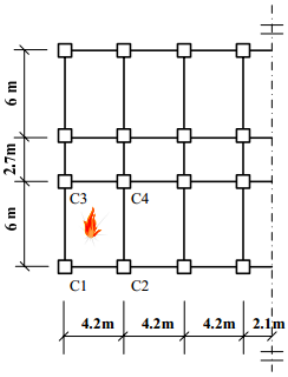

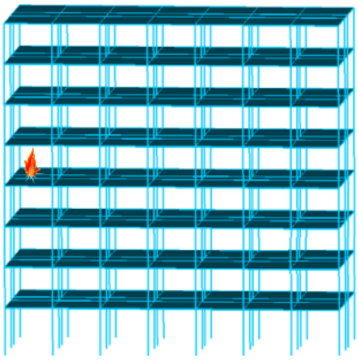

(a) Plan layout (b) Global structural model

Fig. 7 8-story RC frame example

5.2 The simulation for the process of fire-induced progressive collapse

The simulated structural collapse process is shown in Fig. 8, and the axial forces of the four frame columns are given in Fig. 9.

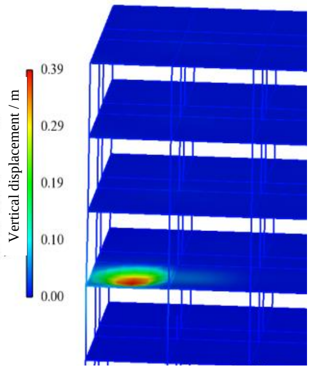

(a) Column C4 (137min)

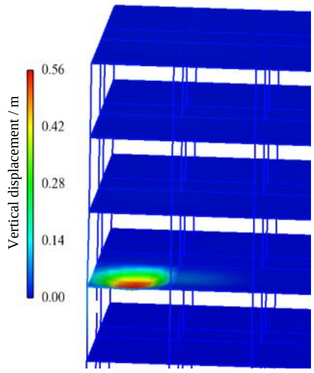

(b) Column C3 (240min)

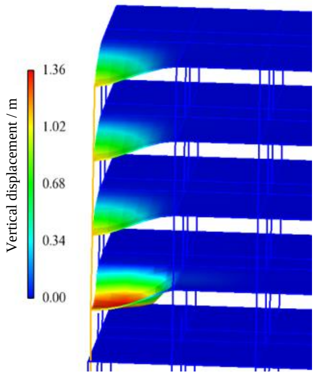

(c) Column C1 (395min)

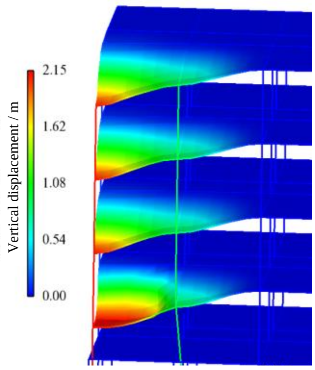

(d) Column C2 (403min)

Fig. 8. The damage of the columns in the 8-story frame.

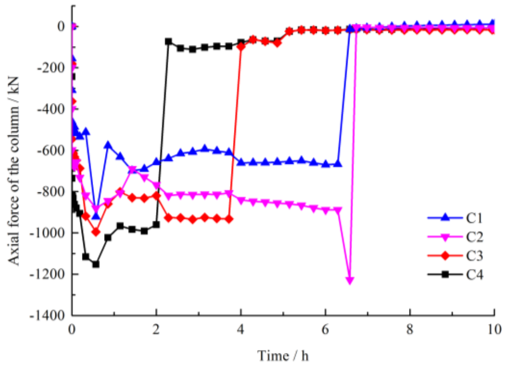

Fig. 9. The axial force of the frame columns subjected to fire.

It can be seen that at the beginning of the fire action, the heated frame columns expands and the axial forces of the columns increase significantly because of the load transferred from the upper floors and the restrained boundary provided by the surrounding structure, as shown in Fig. 9. Failure occurred in Column C4 first at approximately 137 minutes and the deformation of the upper slabs significantly develops, as shown in Fig. 8(a). Meanwhile, the axial forces of Columns C2 and C3 that are at the same planar frame with Column C4 increased, which shows the internal force has been redistributed in the global structure. With the continuous fire development, Column C3 fails suddenly at 240 minutes. At this time, the structure remains stable after two columns damaged which shows that the global structure can absorb the damage of the columns by the internal force redistribution capacity. Failure occurred in Column C1 at 395 minutes. The heated structure cannot carry any more unbalanced gravity load, which causes the large deformation of the surrounding beams and slabs as shown in Fig. 8(c). The damage of Column C1 causes the significant increase of the axial force of adjacent Column C2 and then subsequently damages the Column due to the over-loading. This eventually triggers the progressive collapse of the structure.

6. CONCLUSIONS

An accurate and efficient numerical model is the basis of the design and research on the fire-induced progressive collapse of building structures. This work establishes a numerical analysis model for the fire-induced collapse analysis of RC frame structures. The main conclusions include:

(1) Based on the basic principle of the thermal-mechanical coupled analysis, the material constitutive laws have been built, which considers various high-temperature strain components and the transformation of stress-strain state under different temperature.

(2) A fiber beam model and a layered shell model considering thermal effect have been developed to simulate the mechanical behavior of RC beams (or columns) and slabs subjected to fire. The models are cooperated with the elemental failure criteria by which the fracture of structural members during progressive collapse can be considered. The accuracy of the model has been validated by a series of experiments of members.

(3) A typical 8-story frame structure is analyzed to validate the performance of the proposed model for analyzing the fire-induced progressive collapse of entire structures.

Acknowledgments

The authors are grateful for the financial support received from the National Basic Research Program of China (973 Program) (No. 2012CB719703), the National Natural Science Foundation of China (No. 51208011) and Australian Research Council through an ARC Discovery Project (DP150100606).

REFERENCES

Bratina, S., Saje, M., and Planinc, I. (2007), “The effects of different strain contributions on the response of RC beams in fire.” *Eng.Struct.*, **29**(3): 418–430.

CEN. (2004a). EN 1992-1-1. Eurocode 2: Design of concrete structures. Part 1: General rules and rules for buildings. Brussels: European Committee for Standardization.

CEN. (2004b). EN 1992-1-2. Eurocode 2: Design of concrete structures. Part 1-2: General rules -Structural fire design. Brussels: European Committee for Standardization.

Chen, L.G. (2004), “The experimental research of reinforced concrete slab.” Xi'an University of Architecture and Technology, Xi'an. (in Chinese)

Ellingwood, B.R. (2006), “Mitigating risk from abnormal loads and progressive collapse.” *J. Perform. Constr. Fac.*, **20**(4): 315—323.

Ministry of Public Security of People's Republic of China(2006). GB 50016-2006: Code of Design on Building Fire Protection and Prevention, China Planning Press, Beijing. (in Chinese)

Guo, Z.H. and Shi, X.D. (2003a), Behavior of reinforced concrete at elevated temperature and its calculation, Tsinghua University Press, Beijing. (in Chinese)

Guo, Z.H. and Shi, X.D. (2003a), Reinforced concrete theory and analyse, Tsinghua University Press, Beijing. (in Chinese)

Lie, T.T. and Irwin, R.J. (1993), “Method to calculate the fire resistance of reinforced concrete columns with rectangular cross section.” *ACI Struct. J.*, **90**(1):52-60.

Lim, L. and Wade, C. (2002), Experimental fire tests of two-way concrete slabs. Fire Engineering Research Report, University of Canterbury, New Zealand.

MSC.Software Corporation. User documentation volume A: Theory and user information . www.mscsoftware.com, 2007.

Nan, J.L. (1994), “The experimental research of concrete mechanical properties under the coupling of temperature and stress.” Tsinghua University, Beijing. (in Chinese)

Williams-Leir, G. (1983), “Creep of structural steel in fire: analytical expressions.” *Fire Mater.*, **7**(2): 73-78.

Ye L.P., Lu X.Z., Ma Q.L., Wang X.L., Miao Z.W. (2006), “Nonlinear analytical models, methods and examples for concrete structures subject to earthquake loading.” J. Eng. Mech., 23(Sup. II): 131-140. (in Chinese)

Yi W.j., He Q.F., Xiao Y. (2007), “Collapse performance of RC frame structure.” J. Build. Struct., **28**(5): 104-109. (in Chinese)